An Adaptive Time Series Probabilistic Framework for 4D Trajectory Conformance Monitoring

Dimitrios Sotiriou*, Fotis Kopsaftopoulos† and Spilios Fassois*‡

***Abstract*—Trajectory conformance monitoring is important for future air traffic control for reasons associated with optimal operation, increased safety, and improved efficiency. In this study conformance monitoring is considered with respect to preassigned 4D (space and time) trajectories and their margins (4D contracts), and an adaptive time series probabilistic framework is postulated. Two problems are tackled and proper methods are developed: (a) present conformance monitoring and quality of conformance evaluation via statistical tools, which leads to abnormal event detection, and (b) future conformance monitoring in which conformance is predicted ahead of time allowing for the early initiation of corrective actions. The framework is based on Recursive Integrated AutoRegressive (RIAR) modeling of contract deviations alone, with the underlying dynamics and non-stationarity accounted for. An initial assessment of the performance of the framework is based on two simulation scenarios. Through them, present conformance monitoring is shown to lead to quality assessment and the declaration of an alarm immediately following the emergence of an abnormal event. Future conformance monitoring is shown to lead to an early non-conformance alarm, with the lead time shown to be significantly longer than that achieved by a current probabilistic benchmark scheme.**

***Index Terms*—conformance monitoring, adaptive models, time series models, quality of conformance, trajectory monitoring**

I. Introduction

Aircraft navigation monitoring is a necessary tool for ensuring the safety, security and efficiency of air traffic operations [1]–[3]. It involves the creation and assignment of flight plans to each aircraft with clearances issued by air traffic controllers given the constraints of the Air Traffic Control (ATC) system. In future ATC concepts, these clearances may be based on aircraft-preferred conflict-free trajectories authorized by a centralized ground unit [4]–[6]. With the increased use and density of the air space, an automated ATC function is required to ensure that aircraft adhere to their assigned trajectories. Therefore, the early detection and/or prediction of unacceptable deviations is critical in order to ensure the safe system operation and allow for the initiation of corrective actions when necessary. This function is referred to as conformance monitoring [1]–[3].

*Dimitrios Sotiriou and Spilios Fassois are with the Stochastic Mechanical Systems & Automation (SMSA) Laboratory, Department of Mechanical & Aeronautical Engineering, University of Patras, GR 26504 Patras, Greece, Email: {dimsot,fassois}@mech.upatras.gr Internet: http://www.smsa.upatras.gr. ‡Spilios Fassois is also with the Khalifa University of Science, Technology & Research (KUSTAR), PO Box 127788, Abu Dhabi, UAE. Email: spilios.fassois@kustar.ac.ae.

†Fotis Kopsaftopoulos is with the Structures and Composites Laboratory (SACL), Department of Aeronautics & Astronautics, Stanford University, CA 94305, USA, Email: fkopsaf@stanford.edu

Thus far conformance monitoring has been typically performed by ATC comparing radar data with assigned flight paths [1]. As a result, significant deviations often exist before aircraft non-conformance may be detected. Such deviations are due to limited navigational and pilot tracking capabilities, pilot response and communication issues, surveillance capabilities (radar, GPS, ADS-B and so on), severe weather, airport closure, faults in aircraft systems (on-board sensors, controllers, engines and so on), and other reasons that may cause loss of situational awareness [1]–[3].

The issue of conformance monitoring has been addressed in a number of studies [1]–[3], [7]–[10]. The present state of the art employs relatively simple algorithms where non-conformance is flagged when the observed deviation of an aircraft from its assigned trajectory exceeds some predetermined threshold values. Yet, limited attention has been paid to the task of future conformance monitoring, that is predicting conformance ahead of time. Although several trajectory prediction approaches have been suggested [11]–[14], very few studies treat the issue of future conformance monitoring [15]. Trajectory prediction methodologies may be divided into three categories: nominal, worst case, and probabilistic [11]. Nominal methods predict the aircraft position by propagating the aircraft states into the future without taking into account uncertainties. Worst-case methods assume that an aircraft will perform any of a set of prescribed maneuvers and the worst case one is selected for trajectory prediction. Probabilistic methods predict the future trajectory by taking into account uncertainties. For a review of these methods the reader is referred to [11].

The focus of the present study is on the problem of conformance monitoring with respect to preassigned 4D trajectories (latitude, longitude, altitude, and time) equipped with corresponding 4D margins. This novel concept, referred to as *4-dimensional contract (4D contract)*, was introduced in recent studies [4]–[6], [16], [17] as a step change in future air transport operations by providing a radical and environmentally efficient solution to the airspace management problem. The ground segment of the system is in charge of generating conflict-free 4D trajectories (4D contracts) and corresponding margins according to demand, airspace/airport capacity, and aircraft tracking capabilities. Then, the complete 4D contracts are assigned to aircraft that have to follow them based on their piloting and on-board control systems. In this context, the conformance of any flown 4D trajectory with respect to the assigned contract has to be continuously monitored by the ATC and on-board systems.

In the present study two specific problems are considered

IEEE Transactions on Intelligent Transportation Systems, Vol. 17(6), pp. 1606-1616, 2016.

and tackled within a postulated *adaptive time series probabilistic framework*:

A. *Present conformance monitoring* in which a flown trajectory is monitored via the on-line calculation of the along-track, cross-track, and altitude aircraft deviations with respect to its assigned 4D contract. In this context the *statistical quality of conformance* is evaluated and monitored. This not only provides a statistical measure of the quality of conformance, but also leads to the prompt detection of abnormal or hazardous events that may lead to degraded conformance or loss of conformance.

B. *Future conformance monitoring* in which trajectory conformance is *predicted* ahead of time allowing for the initiation of corrective actions *prior* to the occurrence of unacceptable deviations. In this context future deviations are predicted for a proper prediction horizon, while corresponding probabilities of non-conformance are calculated and continuously provided.

The *main elements* of the postulated probabilistic framework are: (i) integrated adaptive time series models capable of optimally representing the time-varying nature of contract deviation dynamics under uncertainty, (ii) recursive model estimation techniques for on-line (in-flight) parameter estimation, (iii) model-based prediction of future deviations, and (iv) statistical decision making and statistical process control. This framework accounts for uncertainties, such as environmental conditions (turbulence, wind, and so on), aircraft navigation capabilities and tracking errors, and surveillance errors. In addition, the adaptive time series models are capable of effectively representing the deviation time–varying dynamics and accounting for non-stationarity.

A significant feature of the proposed framework lies with the simplification of the prediction function. Indeed, instead of predicting the aircraft flown trajectory, the framework is based on predicting the trajectory *deviations*, that is the difference between the assigned (by the ground segment) 4D contract and the actually flown trajectory. This way there is no need for using aircraft intent information (such as planned by a specific aircraft flight trajectory) in the prediction function.

In addition, there is no need for accounting for the aircraft kinematic equations in the prediction, which would necessitate the use of elaborate techniques and time consuming algorithms [8], [10], [13]–[15]. As a result, the postulated framework is based on compact (small in size) and computationally simple adaptive time-varying models that can be effectively estimated on-line. The present work constitutes the extension and refinement of a preliminary study [18] by two of the authors, which was based on conventional Recursive AutoRegressive (RAR) models, instead of their presently employed integrated versions (that is Recursive Integrated AutoRegressive (RIAR) models). The new models are somewhat more elaborate and lead to improved modeling and prediction capabilities.

The performance of the present and future conformance monitoring is assessed via two simulated scenarios employing a Boeing 737 aircraft. The future conformance monitoring results are also contrasted to those obtained by a standard probabilistic method based on trajectory prediction [19], [20].

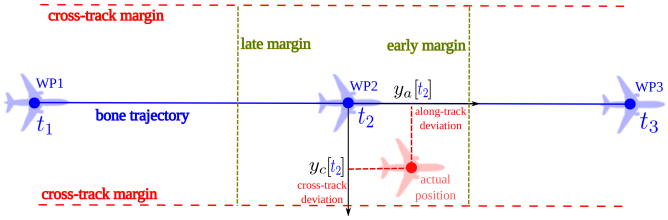

Fig. 1. Schematic representation of the contract bone trajectory and the contract margins, along with the along-track and cross-track deviations [18].

The paper is organized as follows: A preamble is presented in Section II, while the conformance monitoring framework is postulated in Section III. The adaptive time series modeling framework is presented in Section IV. Simulation results and assessment are presented in Section V, while concluding remarks are summarized in Section VI.

II. Preamble

A. The 4D contract

The main element of a 4D contract is the *bone trajectory*, which is the element of the contract that should be as close as possible to the actually flown trajectory [6], [17]. Thus, aircraft performance, weather, optimized flight procedures, and other constraining factors need to be taken into account during bone trajectory generation. The bone trajectory consists of a number of 4D waypoints (WPs) that define its geometry, along with corresponding 4D margins. Intermediate points may be also generated via great circle interpolation.

For short and mid-term time horizons, the different sources of uncertainty affecting aircraft motion generally cause deviations from the nominal flight path that cannot be neglected. The aircraft must thus monitor their own conformance, and in case of conformance loss, request a new contract. Of course, all contracts involve conflict-free trajectories.

B. Contract deviations

The contract deviations are computed from the distance between the bone trajectory WPs and the actual aircraft position for a specific time instant. Without loss of generality, the present study considers the 3-dimensional case, focusing on along-track and cross-track deviations, thus neglecting altitude deviations. Figure 1 presents a schematic representation of the bone trajectory along with the along-track and cross-track margins and the corresponding deviations. The distance between the bone trajectory WP and the actual aircraft position for a specific time instant is computed and projected onto the bone trajectory along-track and cross-track axes (Figure 1). In order to convert the along-track deviation from distance unit (nmi) to time (s) the nominal bone trajectory velocity is used based on the relation $y_a[t] = d_a[t]/u_g[t]$, with $y_a[t]$ designating the along-track deviation in seconds (s), $d_a[t]$ the along-track deviation in nautical miles (nmi), $u_g[t]$ the nominal bone trajectory ground velocity, and t referring to normalized discrete time, with the corresponding actual time being $(t-1)T_s$ where T_s stands for the sampling period.

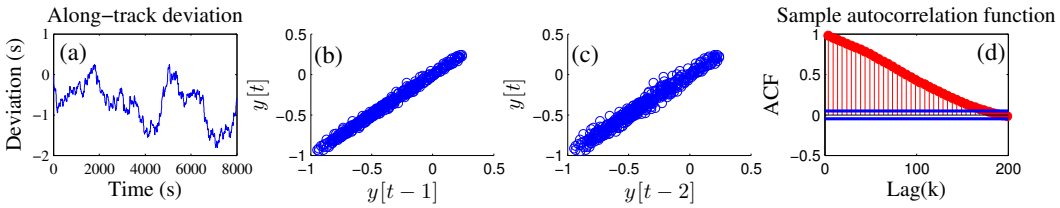

Fig. 2. Indicative deviation dynamics: (a) along-track deviation $y[t]$ versus flight time t; (b) deviation signal $y[t]$ versus $y[t-1]$; (c) $y[t]$ versus $y[t-2]$; and (d) autocorrelation function of along-track deviation signal.

C. Deviation dynamics

Contract deviations are characterized by three important features: (i) uncertainty due to surveillance and measurement errors, (ii) time-varying dynamics due to continuously changing conditions, such as environmental (such as turbulence, wind, gusts, and so on) and flight (such as turns, altitude changes, velocity changes, and so on) conditions, and (iii) homogeneous non-stationarity due to auto-throttle dynamics. Furthermore, it should be pointed out that the deviation dynamics are affected by the aircraft navigational and tracking capabilities as they are determined by the pilot and/or autopilot performance characteristics.

Figure 2 presents an indicative along-track deviation signal $y[t]$ and its preliminary analysis. Figure 2a depicts the signal versus flight time. It is correlated with the aircraft auto-throttle dynamics which dominates over its stochastic component. Figures 2b and 2c present facets of the signal analysis, specifically $y[t]$ versus $y[t-1]$ and $y[t]$ versus $y[t-2]$ correlograms. Both indicate strong dependencies, and thus dynamics. The signal's sample autocorrelation function (ACF) is depicted in Figure 2d, with its linear pattern indicating homogeneous non-stationarity.

III. Conformance Monitoring

A schematic representation of the postulated conformance monitoring framework is provided in Figure 3.

A. Present conformance monitoring

In the context of conformance monitoring, the aircraft trajectory deviations (calculated using surveillance techniques, such as GPS or radar) from the bone trajectory are referred to as *conformance errors* or *residuals* [1]–[3].

B. Statistical quality of conformance monitoring

The quality of conformance (QoC) may be defined as a statistical measure of the aircraft deviations with respect to an assigned 4D contract. Monitoring the QoC may lead to the early detection of abnormal or hazardous events, and may be also considered as a generic health monitoring function. When an aircraft experiences abnormal conditions, such as severe turbulence, winds, or other hazardous events such as system failures, the mean and/or variance of the contract deviations are expected to change. This leads to a statistical decrease in the QoC. Historical flight data for various aircraft types can be used to establish proper and robust statistical QoC measures under various environmental and flight conditions. Towards this end, standard statistical tools such as the $\bar{x}$ and S control charts [21, pp. 230–241] may be employed to statistically monitor the sample mean and standard deviation values, respectively.

As the statistical tools referring to quality assurance require serially uncorrelated observations [21, p. 203], an assumption certainly violated in the case of contract deviations, a proper prior action is necessary. Hence, the measured deviation signals are modeled via time-varying adaptive time series techniques using RIAR models (see Section IV). This type of modeling is necessary to properly account for signal serial correlation. Following this, the statistical quality assurance tools are applied on the *residuals* (one-step-ahead prediction error) signal $e[t+1|t]]$ which fulfills the serial uncorrelatedness assumption.

Using the contract deviation *residual* signal $e[t+1|t]]$, its standard deviation $\sigma_e[t]$ and mean $\mu_e[t]$ are estimated via a non-overlapping sliding window of length m. Then the sample standard deviation $\widehat{\sigma}_e[t]$ and the sample mean $\widehat{\mu}_e[t]$ become the charted values using an S and $\bar{x}$ control chart respectively [21, p. 230]. The average value of the standard deviation $\bar{S}$ may be calculated as $\bar{S} = \text{mean}[\widehat{\sigma}_e^i[t]]$ and in the same way for $\bar{\bar{x}} = \text{mean}[\mu_e^i[t]]$. The upper control limit (UCL), control limit (CL), and lower control limit (LCL) for the S chart are defined as $UCL = B_4\bar{S}$, $CL = \bar{S}$ and $LCL = B_3\bar{S}$, respectively. Similarly, the corresponding $\bar{x}$ chart limits are defined as $UCL = \bar{\bar{x}} + A_3\bar{S}$, $CL = \bar{\bar{x}}$, and $LCL = \bar{\bar{x}} - A_3\bar{S}$. The values of B_3 and B_4 are obtained via the following relations or directly from the statistical tables [21]:

$$B_3 = 1 - \frac{3}{c_4\sqrt{2(m-1)}}, \quad B_4 = 1 + \frac{3}{c_4\sqrt{2(m-1)}} \tag{1}$$

$$A_3 = \frac{3}{c_4\sqrt{m}}, \quad \text{with} \quad c_4 = \frac{4(m-1)}{4m-3}. \tag{2}$$

The control charts constitute a means of evaluating the statistical QoC. Abnormal deviations beyond the established limits (UCL) and (LCL) function as alarms for changes in quality, and are, expectedly, associated with various root events. It is finally noticed that the control limits based on the normality assumption may often be successfully used, unless the population is extremely non-normal [21, p. 203].

C. Future conformance monitoring

Future conformance monitoring, taking uncertainties into account, is based on the statistical confirmation that the along-track and cross-track contract future (at time $t+h$) deviations shall be smaller than the specified contract margins $\delta_i[t+h]$

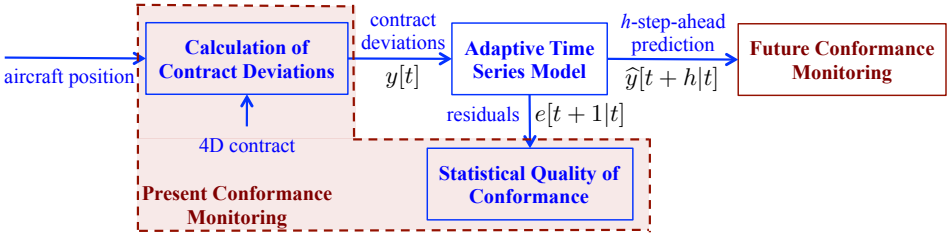

Fig. 3. Schematic representation of the adaptive time series probabilistic framework for present and future conformance monitoring.

(>0), with $i=a$ for the along-track and $i=c$ for the cross-track deviations, in the corresponding direction. This is properly accomplished through a formal statistical hypothesis testing problem of the form:

$$\begin{array}{lcc} H_o: & |y_i[t+h]| \leq \delta_i[t+h] & \text{(conformance)} \\ H_1: & \text{otherwise} & \text{(non-conformance)} \end{array} \quad (3)$$

As the contract deviations $y_i[t+h]$ are not available, their corresponding h-step-ahead predicted values $\widehat{y}_i[t+h|t]$ are employed instead, with $\widehat{y}_i[t+h|t] \sim \mathcal{N}(y_i[t+h], \sigma^2_{y_i}[t+h])$ [22, pp. 131–135]. The variance $\sigma^2_{y_i}[t+h]$ is generally unknown, but may be estimated (see Equation 15). Assuming negligible variability of the estimated variance $\widehat{\sigma}^2_{y_i}[t+h|t]$ this leads to the following decision making mechanism (conservative decision with maximum Type I error probability α, that is probability of accepting the non-conformance hypothesis when the conformance hypothesis is actually true). Defining:

$$Z_A = \frac{\widehat{y}_i[t+h|t] - \delta_i[t+h]}{\widehat{\sigma}_{y_i}[t+h|t]} \quad (4)$$

$$Z_B = \frac{\widehat{y}_i[t+h|t] + \delta_i[t+h]}{\widehat{\sigma}_{y_i}[t+h|t]} \quad (5)$$

decision making is based on:

$$\begin{array}{ccc} Z_A < Z_{1-\alpha}\ (\widehat{y}_i[t+h|t] > 0) & \Rightarrow & H_o \text{ is accepted} \\ Z_B > Z_\alpha\ (\widehat{y}_i[t+h|t] < 0) & \Rightarrow & H_o \text{ is accepted} \\ \text{Else} & \Rightarrow & H_1 \text{ is accepted} \end{array} \quad (6)$$

with $Z_{1-\alpha}$ designating the standard normal distribution's α critical point.

The conditional probability density function of the h-step-ahead deviation $y[t+h] \sim \mathcal{N}(\widehat{y}[t+h|t], \sigma^2_{\widehat{y}}[t+h|t])$ is depicted in Figure 4, with $\delta[t+h]$ the specified contract margin. The estimated probability of non-conformance $P(NC)$ is equal to the sum of probabilities indicated by the two shaded areas in Figure 4.

IV. Adaptive Time Series Modeling

The time-varying nature of the deviation signal characteristics necessitates the use of an appropriate *integrated adaptive* model structure. The model parameters should continuously adapt to the underlying dynamics, and compensate for non-stationarity. In view of the above, an adaptive scheme that is based on the Recursive Integrated AutoRegressive (RIAR) modeling of the contract deviations is postulated. The adaptability of the parameters is achieved via the time-dependent recursive model structure. The homogeneous non-stationarity is compensated by the integrated part, which corresponds to an initial differencing of the signal [22].

An RIAR model is of the following form:

$$(1-\mathcal{B})^d \cdot A(\mathcal{B},t) \cdot y[t] = e[t], \quad e[t] \sim \mathcal{N}(0, \sigma^2_e[t])$$

$$A(\mathcal{B},t) = 1 + a_1[t]\cdot\mathcal{B} + a_2[t]\cdot\mathcal{B}^2 + \ldots + a_{na}[t]\cdot\mathcal{B}^{na} \quad (7)$$

with $y[t]$ being the along-track or cross-track deviation signal modeled, and $e[t]$ an (unobservable) uncorrelated (white) *innovations* sequence with zero mean and variance $\sigma^2_e[t]$. $\mathcal{B}$ designates the backshift operator, defined such that $\mathcal{B}^i \cdot y[t] = y[t-i]$, $a_i[t]$ the i-th AR parameter at time t, and na the AutoRegressive (AR) order (assumed to be invariant). $A(\mathcal{B},t)$ represents the AR polynomial and $\mathcal{N}(\cdot,\cdot)$ stands for Normally Independently Distributed with the indicated mean and variance. The $(1-\mathcal{B})^d$ term corresponds to the integrated part (d represents the integration order) that accounts for the homogeneous non-stationarity. This model is designated as RIAR(na,d).

The RIAR model structure (that is the orders na and d) may be predetermined based on historical data for various aircraft types. This is accomplished via a modeling strategy consisting of the successive fitting of models to aircraft-specific historical flight data until a candidate model structure is selected.

The estimation of the model parameter vector $\boldsymbol{\theta}[t] = [a_1[t] \;\; a_2[t] \;\; \ldots \;\; a_{na}[t]]^T$ is based on minimization of the *weighted least squares criterion* [23, pp. 363–368], [24, p. 324]:

$$\widehat{\boldsymbol{\theta}}[t] = \arg\min_{\boldsymbol{\theta}[t]} \sum_{\tau=1}^{t} \lambda^{t-\tau} \cdot e^2[\tau, \boldsymbol{\theta}^{\tau-1}], \quad \text{with} \quad (8)$$

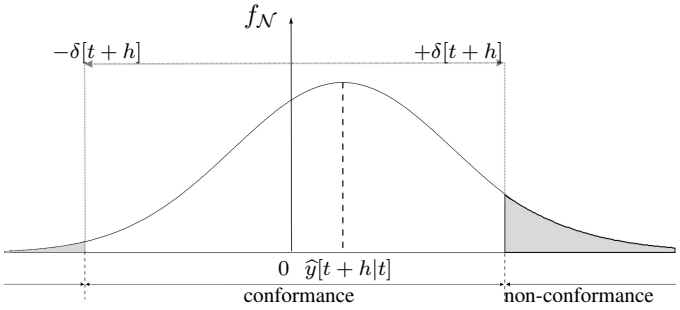

Fig. 4. Conditional probability density function of the h-step-ahead deviation $y[t+h]$ with mean value $\widehat{y}[t+h|t]$ and variance $\sigma^2_{\widehat{y}}[t+h|t]$. The future probability of non-conformance $P(NC)$ is the sum of probabilities indicated by the shaded area. $\delta[t+h]$ designates the specified contract margin.

$$e[t,\boldsymbol{\theta}^{t-1}] = e[t|t-1] = A(\mathcal{B},t)\cdot\underline{y}[t] = \underline{y}[t] - \sum_{i=1}^{na} a_i[t]\cdot\underline{y}[t-i] \tag{9}$$

designating the model's one-step-ahead prediction error (residual) for which the prediction is computed using the model parameters at time $t-1$. Note that the hat designates estimator/estimate, $\arg\min$ the minimizing argument, and $\underline{y}[t] = (1-\mathcal{B})^d \cdot y[t]$ is the differenced signal. Bold face upper/lower case symbols designate matrix/column vector quantities, respectively.

The term $\lambda^{t-\tau}$ is a weighting function that, for $\lambda \in (0,1)$ (λ is referred to as the *forgetting factor*), assigns more weight to more recent deviations. A decreasing value of λ results in an increasing adaptability of the estimator (its ability to track the evolution in the dynamics). Yet, at the same time, estimation accuracy decreases, as the estimator covariance increases [23, pp. 381–382]. Therefore, the selection of λ is crucial, as it represents the basic trade-off between tracking ability in the dynamics and achievable parameter accuracy. The minimization of (8) leads to the Recursive Least Squares (RLS) algorithm (Matlab function *rarx.m*) [23, pp. 363–369]:

$$\widehat{\boldsymbol{\theta}}[t] = \widehat{\boldsymbol{\theta}}[t-1] + \boldsymbol{k}[t]\cdot\widehat{e}[t|t-1] \tag{10}$$

$$\widehat{e}[t|t-1] = \underline{y}[t] - \widehat{\underline{y}}[t|t-1] = \underline{y}[t] - \boldsymbol{\phi}^T[t]\cdot\widehat{\boldsymbol{\theta}}[t-1] \tag{11}$$

$$\boldsymbol{k}[t] = \frac{\boldsymbol{P}[t-1]\cdot\boldsymbol{\phi}[t]}{\lambda + \boldsymbol{\phi}^T[t]\cdot\boldsymbol{P}[t-1]\cdot\boldsymbol{\phi}[t]} \tag{12}$$

$$\boldsymbol{P}[t] = \frac{1}{\lambda}\cdot\left(\boldsymbol{P}[t-1] - \frac{\boldsymbol{P}[t-1]\cdot\boldsymbol{\phi}[t]\cdot\boldsymbol{\phi}^T[t]\cdot\boldsymbol{P}[t-1]}{\lambda + \boldsymbol{\phi}^T[t]\cdot\boldsymbol{P}[t-1]\cdot\boldsymbol{\phi}[t]}\right) \tag{13}$$

with $\widehat{\underline{y}}[t|t-1]$ indicating one-step-ahead prediction of the signal at time t made at time $t-1$ and the term $\widehat{e}[t|t-1] \equiv e[t,\widehat{\boldsymbol{\theta}}[t-1]]$ is the corresponding prediction error. $\boldsymbol{k}[t]$ stands for the adaptation gain and $\boldsymbol{P}[t]$ for the model parameter covariance matrix. $\boldsymbol{\phi}[t] = \left[1\ \underline{y}[t-1]\ \underline{y}[t-2]\ \ldots\ \underline{y}[t-na]\right]^T$ is the regression vector. The time-varying innovations variance $\sigma_e^2[t]$ may be estimated via a window of length m that slides over the prediction error sequence, that is:

$$\widehat{\sigma}_e^2[t] = \frac{1}{m}\sum_{t-m}^{t}\widehat{e}^2[t|t-1]. \tag{14}$$

At each time instant t the estimated RIAR(na,d) model parameter vector $\widehat{\boldsymbol{\theta}}[t]$ is employed for the estimation of the h-step-ahead prediction $\widehat{y}[t+h|t]$ of the contract deviations signal, with $\widehat{y}[t+h|t] \sim \mathcal{N}(y[t+h],\sigma_y^2[t+h])$ [22, pp. 131–135]. Once the predicted value of the signal $\widehat{y}[t+h|t]$ is available, the prediction error variance is:

$$\sigma_y^2[t+h|t] = \mathrm{Var}[e[t+h|t]] = \sum_{j=0}^{h-1} G_j^2[t]\cdot\sigma_e^2[t] \tag{15}$$

where $e[t+h|t]]$ is the prediction error sequence, $\sigma_e^2[t]$ is the residual variance estimated as in (14), and $G_j[t]$ the time-varying Green's function coefficients [25, pp. 314–325]:

$$G(B,t) = G_0[t] + G_1[t]\cdot\mathcal{B} + G_2[t]\cdot\mathcal{B}^2 + \ldots = 1/\bar{A}(\mathcal{B},t) \tag{16}$$

TABLE I
SIMULATION DETAILS

Aircraft type	Boeing 737–500 (JSBSim simulator)
Flight duration	7999 s
Cruise speed	0.74 Mach
Turbulence	high

TABLE II
THE 4D CONTRACT

Number of WPs	23
WPs altitude	FL300
WPs distance	349.2 s (40 nmi)
Heading hold	36.5^o
Along-track margin	$\delta_a = 25$ s (early/late margins)
Cross-track margin	$\delta_c = 1.49$ nmi (left/right margins)

$$\text{where}\quad (1-\mathcal{B})\cdot A(\mathcal{B},t) := \bar{A}(\mathcal{B},t). \tag{17}$$

It is important to mention that due to the time-varying model parameters, the Green's function coefficients are calculated considering that the backshift operator obeys a *non-commutative ("skew") multiplication algebra* ("$\circ$"), defined such that $\mathcal{B}^i\circ\mathcal{B}^j = \mathcal{B}^{i+j}$, $\mathcal{B}^i\circ y[t] = y[t-i]\cdot\mathcal{B}^i$. For details the reader is referred to [26]. Using the above skew multiplication operation:

$$\begin{aligned} G_0[t] &= 1, \quad G_1[t] = \bar{a}_1[t]\cdot G_0[t] \\ &\vdots \\ G_j[t] &= \bar{a}_1[t-(j-1)]\cdot G_{j-1}[t] + \ldots \\ &+ \bar{a}_{na}[t-(j-na)]\cdot G_{j-na}[t]. \end{aligned} \tag{18}$$

The interval predictions of $y[t+h]$ made at time t are then (at the α risk level):

$$\widehat{y}[t+h|t] \pm Z_{1-\frac{\alpha}{2}}\cdot\widehat{\sigma}_y[t+h|t] \tag{19}$$

with $Z_{1-\frac{\alpha}{2}}$ designating the normal distribution's $1-\frac{\alpha}{2}$ critical point.

V. SIMULATION RESULTS & ASSESSMENT

An initial assessment of the postulated framework is based on two simulation scenarios for a Boeing 737 (B737) aircraft flying in the cruise regime. The simulations are conducted using the JSBSim flight simulator, which is an open source non-linear flight dynamics environment [27]. The simulation details and the 4D contract are presented in Tables I and II, respectively. The obtained results are compared with those based on a benchmark nominal probabilistic trajectory prediction method [19], [28]. In this method the predicted aircraft position is calculated by propagating the current aircraft state vector into the future along a single trajectory and inserting pre-specified confidence intervals based on historical data and Monte Carlo simulations [19], [28].

In the context of the postulated framework the selection of both the along-track and cross-track deviation RIAR model structures is based on the Error Sum of Squares/Signal Sum of Squares (ESS/SSS) criterion that describes the predictive ability of the model for a prediction horizon of $h = 36$ (36-step-ahead or 180 s). This is selected as an appropriate

TABLE III
ADAPTIVE MODEL ESTIMATION DETAILS

Prediction horizon	$h = 1$ (present)	$h = 36$ (future)
Along-track model RIAR$(15, 1)$	$\lambda = 0.999$	$\lambda = 0.999$
Cross-track model RIAR$(30, 1)$	$\lambda = 0.999$	$\lambda = 0.999$
Sampling period	$T_s = 5$ s	
Residual variance estimation	Moving window length $m \in [2, 60]$	
RLS estimation method [23, pp. 363–369].		

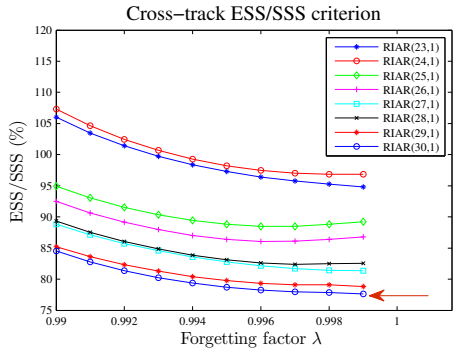

Fig. 5. Cross-track deviation RIAR modeling: model structure selection criterion for a prediction horizon of 180 s ($h = 36$).

mid-term horizon, providing good prediction accuracy and sufficient reaction time (in case the latter is needed). It may be modified, bearing in mind that (for all prediction algorithms) accuracy improves for shorter horizons, but deteriorates for longer ones [22]. The ESS/SSS criterion (for $h = 1$ the ESS coincides with the Residual Sum of Squares–RSS) is employed in an off-line procedure using historical flight data. AR orders na up to 30 and forgetting factor values $\lambda \in [0.93, 0.999]$ (incremental step of 0.001) are presently considered. Figure 5 depicts the ESS/SSS criterion for various combinations of λ and na, indicating the model which provides the best fit (achieves the minimum ESS/SSS value). The selected RIAR models and estimation details are presented in Table III.

A. Simulation scenario A

The scenario involves a cruise flight complying with its contract when an fault in the heading controller occurs at $t_d = 5945$ s causing a constant heading bias. This results in non-conformance at time $t_v = 6166$ s when the cross-track margin $\delta_c = 1.49$ nmi is exceeded.

1) Adaptive time series modeling: For this simulation scenario, RIAR$(15, 1)$ and RIAR$(30, 1)$ models have been used for modeling the along-track and cross-track deviation signals, respectively (Table III). During the simulations the structural form (model order and forgetting factor) of these models is kept constant, while their parameters are being estimated recursively throughout the flight.

2) Present conformance monitoring: Figure 6 presents the along-track and cross-track deviations. The vertical dashed lines indicate the time instants t_d and t_v in which the heading deviation is initiated and the contract is violated, respectively. It is evident that the cross-track contract margin is exceeded at time $t = 6166$ s. Notice that the along-track deviation stays less than 4 s, which is significantly lower than the horizontal

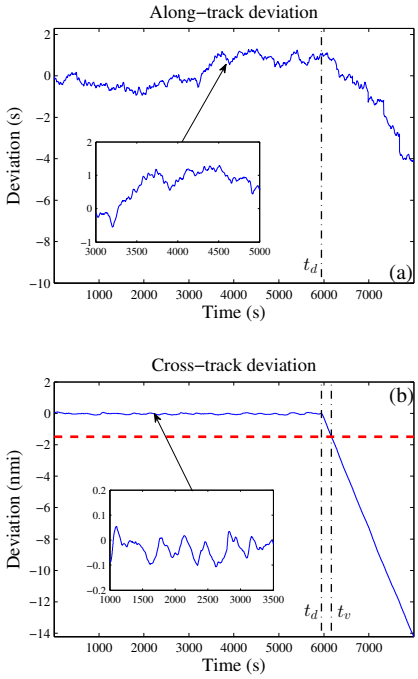

Fig. 6. Scenario A: present conformance monitoring. Aircraft contract deviations evolution: (a) along-track deviation in seconds and (b) cross-track deviation in nautical miles, depicted in blue. The horizontal red dashed line designates the cross-track contract margin.

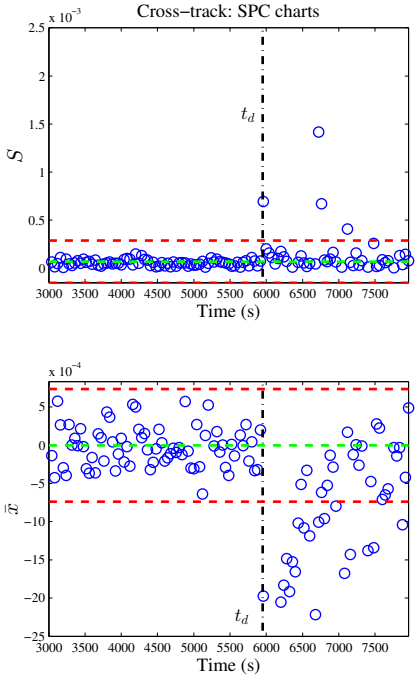

Fig. 7. Scenario A: statistical quality of conformance monitoring and event detection via the (a) S-chart and (b) $\bar{x}$-chart ($m = 8$).

margin, throughout the cruise duration. The oscillatory behavior of the cross-track deviation signal is due to the heading controller dynamics that, evidently, have a significant effect on the contract deviation dynamics.

3) Quality of conformance monitoring: Figure 7 demonstrates the ability of the method to indicate that the quality of conformance has been degraded once the underlying event

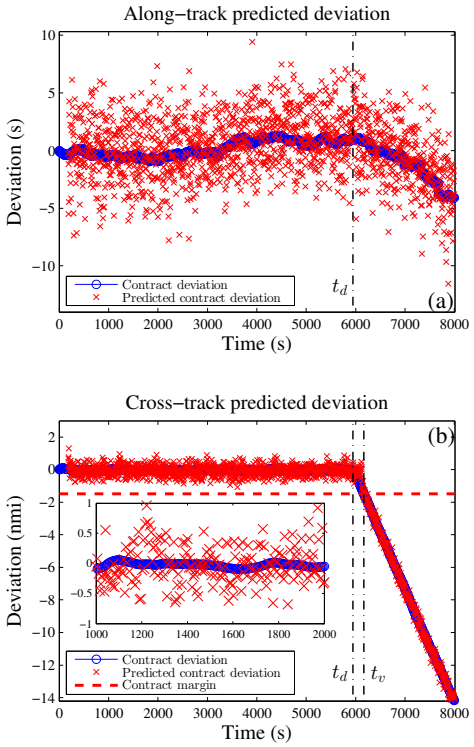

Fig. 8. Scenario A: nominal probabilistic method based predictions (prediction horizon of 180 s): actual versus predicted contract deviations for the (a) along-track and (b) cross-track deviations. The horizontal dashed line designates the contract margin.

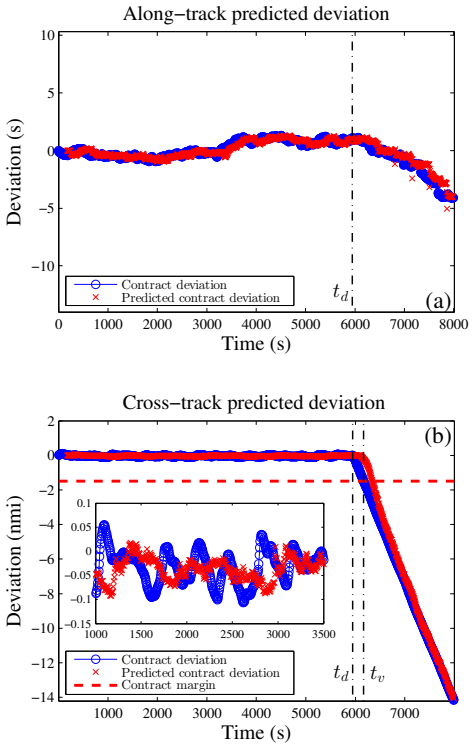

Fig. 9. Scenario A: adaptive RIAR model based predictions (prediction horizon of 180 s): actual versus predicted contract deviations for the (a) along-track and (b) cross-track deviations. Contract margins are depicted in dashed red lines.

occurs (fault in the heading controller). The results are excellent, as the method is able to provide an *immediate* alert of the cross-track induced conformance quality degradation and event occurrence. The method is able to provide an alert within the first 8 seconds (depends on moving window length m) from the occurrence of the event.

4) Future conformance monitoring: The predicted along-track and cross-track deviations, obtained by the benchmark nominal probabilistic method for a prediction horizon of 180 s ($h = 36$), are depicted in Figure 8. Notice that for the along-track case the predicted contract deviations cannot track accurately the actual contract deviation signal, as the actual heading of the aircraft is used into the computations. Figure 9 presents the adaptive time series RIAR$(15, 1)$ and RIAR$(30, 1)$ model based (see Table III) predicted contract deviations for a prediction horizon of 180 s. By comparing the resulting predictions obtained by both the methods (Figures 8–9), it is evident that the prediction errors obtained by the adaptive RIAR model based method are significantly lower than those of the nominal probabilistic method.

Finally, the probabilities of non-conformance for a prediction horizon of 180 s are, for both methods, presented in Figure 10. The nominal probabilistic method achieves a cross-track probability of non-conformance $P(NC) = 0.95$ at flight time $t_{0.95} = 6404$ s. The same probability is achieved by the postulated adaptive time series based method at time $t_{0.95} = 6278$ s, that is 126 seconds *earlier* than the nominal probabilistic method. Hence, the superiority of the postulated approach over the benchmark state-of-the-art method is evident.

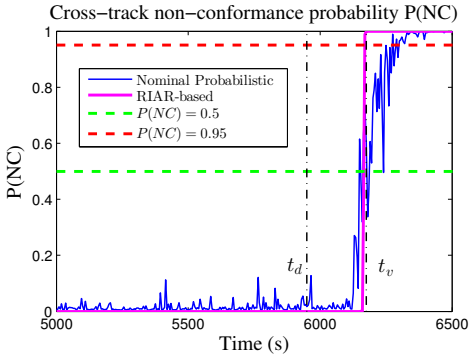

Fig. 10. Scenario A: Probability of non-conformance for the cross-track contract deviations versus flight time for the nominal probabilistic and adaptive statistical time series methods (prediction horizon of 180 s).

B. Simulation scenario B

This scenario involves a B737 aircraft during cruise flight complying with its contract when a linearly increasing heading deviation and an auto-throttle fault affecting the aircraft velocity occur at $t_d = 5945$ s. This results in non-conformance, as the along-track and cross-track margins are exceeded at times 6230 and 6160 seconds, respectively. The contract and simulation details are presented in Tables II and I, respectively.

1) Adaptive time series modeling: Similarly to Scenario A, RIAR$(15, 1)$ and RIAR$(30, 1)$ models have been used for the along-track and cross-track deviation signals, respectively.

2) Present conformance monitoring: Figure 11 shows the along-track and cross-track deviations. It is evident that both the along-track and cross-track contract margins are exceeded,

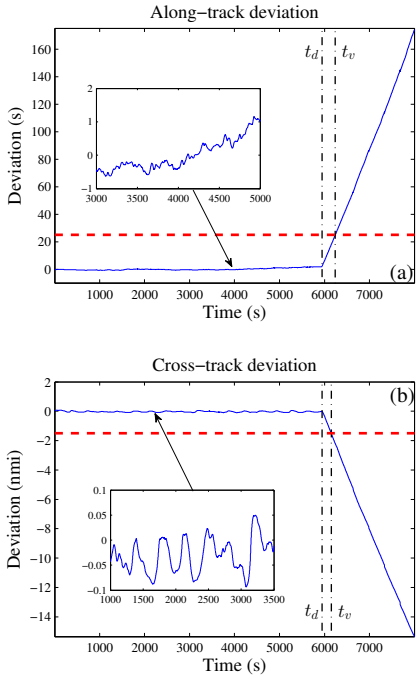

Fig. 11. Scenario B: present conformance monitoring. Contract deviations for heading and velocity faults initiated at 1950 s: (a) along-track deviation and (b) cross-track deviation. The vertical dashed lines indicate the time instants t_d and t_v in which the events occur and the contract is violated, respectively. The horizontal dashed lines designate the contract margins.

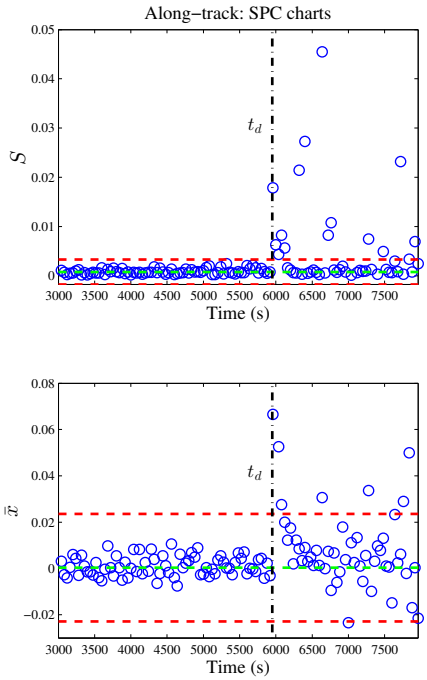

Fig. 12. Scenario B: along-track statistical quality of conformance monitoring (QoC) and event detection via the (a) S-chart and (b) $\bar{x}$-chart ($m = 20$).

with the latter occurring first.

3) Quality of conformance monitoring: Figure 12 demonstrates the ability of the method to indicate that the QoC has been degraded once the fault occurs for the case of the along-track deviation. The results are excellent, as the method is able to provide an *immediate* alert of the conformance quality degradation. The method provides an alert within the first 20 seconds from the initiation of the fault. Also, notice that the monitored statistical quantity quickly returns inside the statistical limits, as the adaptive model compensates for the induced faults and corresponding deviations, and thus the residual standard deviation decreases. The S and $\bar{x}$ control charts in the case of cross-track deviation present analogous results and are omitted for the sake of brevity.

4) Future conformance monitoring: The predicted along-track and cross-track deviations, and their ± 3 standard deviation (99%) confidence intervals, obtained by the nominal probabilistic method for a prediction horizon of 180 s ($h = 36$), are depicted in Figure 13. Figure 14 presents the corresponding adaptive time series based (see Table III) predicted deviations for an horizon of 180 s and their ± 3 standard deviation confidence intervals. It is evident that the adaptive model provides significantly narrower confidence intervals for the predicted deviations in both cases (compare with Figure 13).

By comparing the resulting prediction errors obtained by both methods (Figures 13–14), it is evident that the prediction errors obtained by the adaptive RIAR model based method are significantly lower than the corresponding of the nominal probabilistic method. The confidence intervals obtained by the nominal probabilistic method for the along-track are ± 5 s for

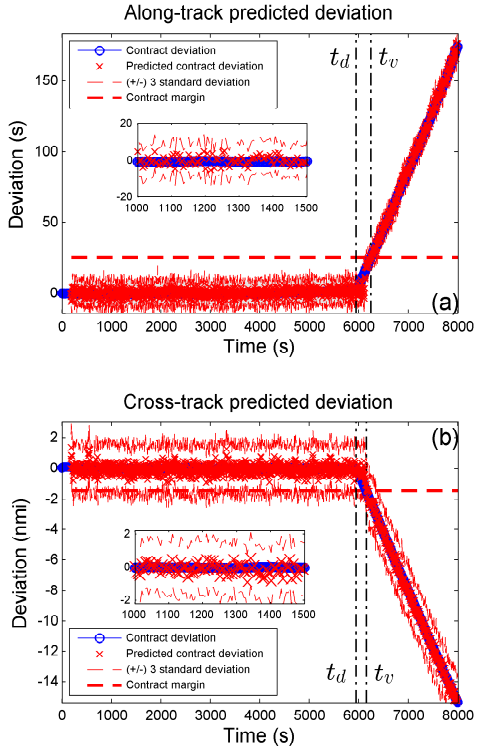

Fig. 13. Scenario B: nominal probabilistic method based deviation predictions (prediction horizon of 180 s): actual versus predicted deviations along with the corresponding ± 3 standard deviation confidence intervals (dashed red lines) for the (a) along-track and (b) cross-track deviations. The vertical dashed lines indicate the time instants t_d and t_v in which the heading deviation is initiated and the contract is violated, respectively.

a prediction horizon of 180 s. On the other hand, the adaptive

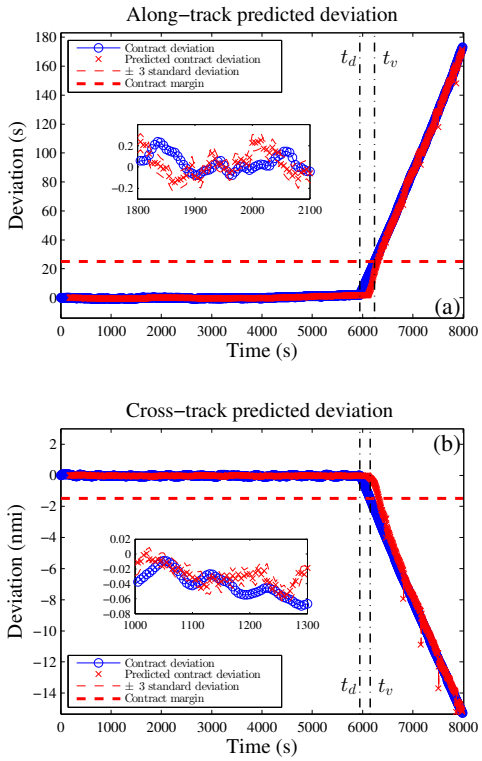

Fig. 14. Scenario B: adaptive RIAR model based predictions (prediction horizon of 180 s): actual versus predicted deviations along with the corresponding ± 3 standard deviation confidence intervals (dashed red lines) for the (a) along-track and (b) cross-track deviations. The vertical dashed lines indicate the time instants t_d and t_v in which the heading deviation is initiated and the contract is violated, respectively.

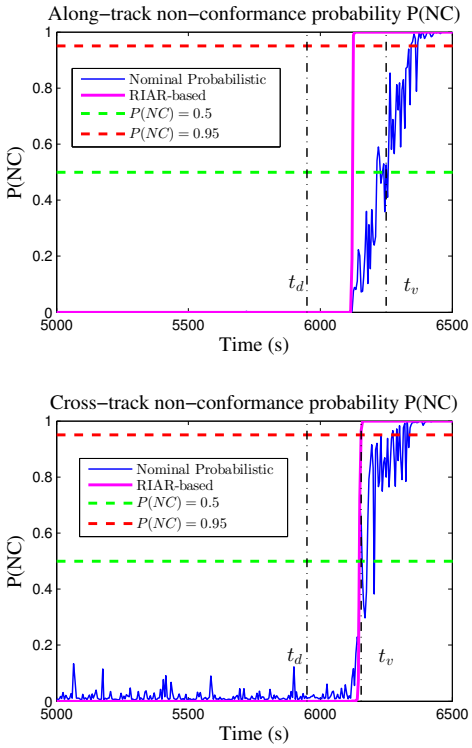

Fig. 15. Scenario B: Probability of non-conformance for the along-track and cross-track contract deviations versus flight time for the nominal probabilistic and adaptive statistical time series methods (prediction horizon of 180 s).

time series model gives significantly narrower confidence intervals at the level of ± 0.026 s before the deviation occurs. The confidence intervals for the cross-track predicted deviation are ± 0.534 nmi while the corresponding obtained by the adaptive RIAR model are at the level of ± 0.003 nmi.

Finally, the probability of non-conformance for a prediction horizon of 180 s is for both methods presented in Figure 15. The nominal probabilistic method achieves an along-track probability of non-conformance $P(NC) = 0.95$ at flight time $t_{0.95} = 6345$ s. The same probability is achieved by the adaptive time series based method at time $t_{0.95} = 6126$ s, which is 219 seconds *earlier*. Hence, the adaptive model based method provides a warning significantly earlier before violation occurs. On the other hand, the nominal probabilistic method yields a probability of cross-track non-conformance $P(NC) = 0.95$ at time $t_{0.95} = 6272$ s. This probability is achieved by the adaptive time series based method at time $t_{0.95} = 6154$ s, which is 118 seconds *earlier*. It is evident from Figure 15 that the adaptive method is capable of providing a significantly earlier violation warning than the nominal probabilistic method, especially for the along-track case where it issues an alert almost 4 minutes earlier.

VI. Concluding Remarks

An adaptive time series probabilistic framework for 4D conformance monitoring was postulated. The framework is based on adaptive Recursive Integrated AutoRegressive (RIAR) time series modeling, model based prediction, and statistical decision making. The RIAR models account for non-stationarity while effectively exploiting the underlying dynamics. Based on this framework, methods for *present conformance monitoring*, along with *quality of conformance monitoring*, as well as *future conformance monitoring* were developed. Beyond its inherent accounting of the underlying dynamics and uncertainties, the postulated framework offers a number of advantages, including conceptual and computational simplicity (no use of kinematic and related equations), prediction of only the aircraft deviation signal (instead of the aircraft trajectory), and no need for incorporating aircraft intent information in the prediction function. The statistical quality of conformance unit also serves as a generic health monitoring and abnormal event detection function.

The performance of the framework was assessed via two simulation scenarios. In present conformance monitoring, conformance quality was shown to be effective and an alarm was issued immediately following the emergence of an abnormal event. In future conformance monitoring, the proposed method was shown to provide a non-conformance alarm significantly earlier than a nominal probabilistic method. Current research focuses on various extensions and the complete validation and assessment of the adaptive time series probabilistic framework via additional flight scenarios and Monte Carlo simulations.

Acknowledgment

The authors wish to acknowledge the support by the European Commission (FP7 Project No. 266296, “4-Dimensional Contracts: Guidance and Control” (4DCo-GC)). They also

wish to thank all project partners for their support and useful discussions, as well as the Editor, Professor Fei-Yue Wang, and three anonymous referees who provided constructive comments that helped in further improving the manuscript.

REFERENCES

[1] T. G. Reynolds and R. J. Hansman, "Investigating conformance monitoring issues in air traffic control using fault detection approaches," Department of Aeronautics & Astronautics, Massachusetts Institute of Technology, Cambridge, MA 02139, U.S.A., Report ICAT-2003-5, November 2003.

[2] ——, "Analyzing conformance monitoring in air traffic control using fault detection approaches and operational data," in *Proceedings of AIAA Guidance, Navigation, and Control Conference and Exhibit*, Austin, Texas, U.S.A., August 2002.

[3] ——, "Investigating conformance monitoring issues in air traffic control using fault detection techniques," *Journal of Aircraft*, vol. 42, no. 5, pp. 1307–1317, Sep. 2005. [Online]. Available: http://arc.aiaa.org/doi/abs/10.2514/1.10055

[4] "Innovative future air transport system (IFATS) conclusions and findings," Tech. Rep., March 2007.

[5] "Concept of operations for the next generation air transportation system," Joint Planning and Development Office, Washington D.C., Tech. Rep. Version 3.0, February 2010.

[6] "4DCo-GC annex 1. description of work," Tech. Rep. V1.2, June 2010. [Online]. Available: http://www.4dcogc-project.org

[7] C. E. Seah, A. Aligawesa, and I. Hwang, "An algorithm for conformance monitoring in air traffic control," in *Guidance, Navigation, and Control and Co-located Conferences*. American Institute of Aeronautics and Astronautics, Aug. 2009. [Online]. Available: http://dx.doi.org/10.2514/6.2009-6170

[8] ——, "Algorithm for conformance monitoring in air traffic control," *Journal of Guidance, Control, and Dynamics*, vol. 33, no. 2, pp. 500–509, Aug. 2010. [Online]. Available: http://dx.doi.org/10.2514/1.44839

[9] K. Lee and Y. Fukuda, "A Bayesian approach for conformance monitoring," in *Proceedings of the 11th AIAA Aviation Technology, Integration, and Operations (ATIO) Conference*, Virginia Beach, U.S.A., September 2011.

[10] Y. Fukuda and K. Lee, "Conformance monitoring under uncertainty in trajectory," in *Guidance, Navigation, and Control and Co-located Conferences*. American Institute of Aeronautics and Astronautics, Aug. 2012. [Online]. Available: http://dx.doi.org/10.2514/6.2012-4930

[11] L. C. Yang and J. K. Kuchar, "Review of conflict detection and resolution modeling methods," *IEEE Transactions on Intelligent Transportation Systems*, vol. 1, no. 4, pp. 179–189, December 2000.

[12] W. Liu and I. Hwang, "Probabilistic trajectory prediction and conflict detection for air traffic control," *Journal of Guidance, Control, and Dynamics*, vol. 34, no. 6, pp. 1779–1789, Aug. 2008. [Online]. Available: http://dx.doi.org/10.2514/1.53645

[13] J. L. Yepes, I. Hwang, and M. Rotea, "An intent-based trajectory prediction algorithm for air traffic control," in *Guidance, Navigation, and Control and Co-located Conferences*. American Institute of Aeronautics and Astronautics, Aug. 2005. [Online]. Available: http://dx.doi.org/10.2514/6.2005-5824

[14] ——, "New algorithms for aircraft intent inference and trajectory prediction," *Journal of Guidance, Control, and Dynamics*, vol. 30, no. 2, pp. 370–382, Aug. 2011. [Online]. Available: http://arc.aiaa.org/doi/abs/10.2514/1.26750

[15] Q. M. Zheng and Y. J. Zhao, "Probabilistic approach to trajectory conformance monitoring," *Journal of Guidance, Control, and Dynamics*, vol. 35, no. 6, pp. 1888–1898, Oct. 2012. [Online]. Available: http://dx.doi.org/10.2514/1.53951

[16] C. Le Tallec and A. Joulia, "IFATS: 4D contracts in 4D airspace," in *Proceedings of the AIAA Infotech@Aerospace Conference and Exhibit*, Rohnert Park, California, U.S.A., May 2007.

[17] A. Joulia and C. Le Tallec, "Aircraft 4D contract based operation: the 4DCo-GC project," in *Proceedings of the 11th AIAA Aviation Technology, Integration, and Operations (ATIO) Conference*, Virginia Beach, U.S.A., September 2011.

[18] F. Kopsaftopoulos and S. Fassois, "An adaptive time series framework for aircraft 4d trajectory conformance monitoring," in *Proceedings of the European Control Conference (ECC)*, Zurich, Switzerland, July 2013.

[19] R. A. Paielli and H. Erzberger, "Conflict probability estimation for free flight," *Journal of Guidance, Control, and Dynamics*, vol. 20, no. 3, pp. 588–596, 1997.

[20] M. Prandini, J. Hu, J. Lygeros, and S. Sastry, "A probabilistic approach to aircraft conflict detection," *IEEE Transactions on Intelligent Transportation Systems*, vol. 1, no. 4, pp. 199–220, December 2000.

[21] D. C. Montgomery, *Introduction to Statistical Quality Control*, 4th ed. John Wiley & Sons, Inc., 2001.

[22] G. E. P. Box, G. M. Jenkins, and G. C. Reinsel, *Time Series Analysis: Forecasting & Control*, 3rd ed. Prentice Hall: Englewood Cliffs, NJ, 1994.

[23] L. Ljung, *System Identification: Theory for the User*, 2nd ed. Prentice–Hall, 1999.

[24] T. Söderström and P. Stoica, *System Identification*. Prentice–Hall, 1989.

[25] P. J. Brockwell and R. A. Davis, *Time Series: Theory and Methods*. Springer-Verlag, 1991.

[26] A. G. Poulimenos and S. D. Fassois, "Parametric time-domain methods for non-stationary random vibration modelling and analysis – a critical survey and comparison," *Mechanical Systems and Signal Processing*, vol. 20, pp. 763–816, 2006.

[27] *http://jsbsim.sourceforge.net/*. [Online]. Available: http://jsbsim.sourceforge.net/

[28] H. Erzberger, R. A. Paielli, D. R. Isaacson, and M. M. Eshow, "Conflict detection and resolution in the presence of prediction error," in *Proceedings of the 1st U.S.A./Europe Air Traffic Management R&D Seminar*, Saclay, France, June 1997.

Dimitrios Sotiriou Dimitrios Sotiriou received his Diploma in Mechanical Engineering and Aeronautics from University of Patras, Greece, in 2012. In the same year he joined the Stochastic Mechanical Systems and Automation (SMSA) laboratory as a Research Assistant. His current research interests include system identification, statistical signal processing, and data analysis.

Fotis Kopsaftopoulos Fotis Kopsaftopoulos received his Diploma and Ph.D. in Mechanical Engineering and Aeronautics from University of Patras, Greece, in 2004 and 2012, respectively, where he also served as a Postdoctoral Research Associate in the Stochastic Mechanical Systems and Automation (SMSA) laboratory. Currently, he is a Postdoctoral Scholar in the Structures and Composites Laboratory (SACL) in the Department of Aeronautics and Astronautics at Stanford University. His research interests are in the areas of stochastic system identification, statistical signal processing, structural health monitoring, and intelligent structures and systems. Dr. Kopsaftopoulos has published over 40 technical articles in esteemed journals, books, and conference proceedings. He has participated in various national, international and industrially supported research projects both in Europe and the USA.

Spilios Fassois Professor Fassois received the Diploma in Mechanical Engineering from the National Technical University of Athens (NTUA), Greece (1982), and the M.Sc. and Ph.D. degrees in Mechanical Engineering from the University of Wisconsin-Madison, USA (1984, 1986). He is Professor and Director of the Laboratory for Stochastic Mechanical Systems and Automation (SMSA) at the Mechanical and Aeronautical Engineering Department of the University of Patras. His research interests are on innovative methods for stochastic mechanical, structural and aeronautical systems, with emphasis on statistical time series methods for stochastic identification and Structural Health Monitoring (SHM). He has been Principal Investigator for over 30 research projects funded by industry, the European Commission, and other organizations. He has been the recipient of several awards, and has published over 240 technical articles in international books, major encyclopedias, editorials to Special Issues, survey and research papers in esteemed journal, and conference proceedings. He is active in international short courses on topics such as Structural Health Monitoring and Structural Identification, is program committee member for many international conferences and technical panels, Editorial Board member for major international journals, and organizer/guest editor for four thematic special issues for esteemed international journals.